ESRF	**Experiment title:** **Enzymatic Catalysed Synthesis and Triggered Gelation of Ionic Peptides**	**Experiment number**: **SC-3008**
Beamline: BM02	**Date of experiment**: from: 03 Nov 2010 to: 05 Nov 2010	**Date of report**: 18/02/2011
Shifts: 6	**Local contact(s)**: Cyrille Rochas (email: cyrille.rochas@esrf.fr)	*Received at ESRF:*

Names and affiliations of applicants (* indicates experimentalists):

Dr A. Saiani, Materials Science Centre, the University of Manchester, Centre Grosvenor Street M1 7HS MANCHESTER, UK

Dr J.-B. Guilbaud*, Materials Science Centre, the University of Manchester, Grosvenor Street M1 7HS MANCHESTER, UK

Dr A. Miller, School of Chemical Engineering & Analytical Science, The University of Manchester, PO Box 88 Sackville Street, M60 1QD MANCHESTER, UK

Dr C. Rochas, CERMAV BP 53X 38041 GRENOBLE Cedex 09, FRANCE

Report:

Molecular self-assembly has emerged as a powerful tool for the fabrication of molecular materials with a wide variety of properties. In recent years, considerable advances have been made in using simple oligo-peptides as building blocks due to their propensity to self assemble into ordered supramolecular structures for the production of such novel biomaterials. The potential to trigger the self assembly of these small molecules by an external stimulus (enzyme, light, pH or ionic strength) is attracting increasing attention as a route for the reversible fabrication of soft solid. Recently, we have investigated the possibility of using a protease type enzyme, thermolysin, to catalyse the synthesis of ionic complementary oligo-peptides *via* reverse hydrolysis, which subsequently triggered gelation. Such ionic oligo-peptides are known to readily self-assemble into β-sheet affording rich fibrillar hydrogels.[(1)] While pure FEFK tetra-peptide (F=phenyalanine, E=glutamic acid, K=lysine) did not form gels over the concentration range 0-300 mg mL^{-1}, in the presence of thermolysin (0.3 mg mL^{-1}) gelation was observed over time for initial tetrapeptide concentration $C_0 \geq 100$ mg mL^{-1}. Gelation was assessed using the simple "test-tube tilting" method, which also suggested that the higher C_0, the faster the gelation. This was confirmed by oscillatory rheology measurements which indicated the formation of stiff gel (G'~25 kPa for C_0=300 mg mL_{-1}), with gel strength increasing with C_0. The composition of the samples at discrete time points was monitored both qualitatively and quantitatively by MALDI-TOF MS and HPLC respectively. Results showed that for $C_0 \geq 100$ mg mL_{-1}) the octa-peptide is the dominant product of the reverse-hydrolysis reaction. As the quantity of octa-peptide synthesized increased, self-assembly into anti-parallel β-sheet fibres was observed by ATR-FTIR. Subsequent TEM investigations revealed the formation of a rich and dense fibrillar network resulting from the self-assembly of the oligo-peptide formed.[(2)]

In the present work, we aimed to investigate the kinetics of fibrillar formation and subsequent gelation of enzyme assisted synthesis of oligo-peptides. SAXS experiments were performed to address the structural changes occurring through this enzymatic reaction. In particular the effect of tetrapeptide/enzyme ratio on the kinetics of fibrillar formation was studied and Table 1 summarises the composition of the samples investigated. Simple "test-tube tilting" method indicated that for C_0=50 mg mL^{-1} gelation did not occur over time irrespectively of the enzyme concentration even after one week of incubation, while for C_0=75 mg mL^{-1} an increase in viscosity was observed despite no gel forming after a week. For $C_0 \geq 100$ mg mL^{-1}, a rapid increase in viscosity is observed and self-supported gels formed after 30 min. Visual observation suggested

the higher the initial enzyme concentration the faster the gelation. Likewise, the higher the initial tetrapeptide concentration the faster the gelation. After one week of incubation, HPLC was performed to evaluate the composition of the samples and especially to quantify the amount of octapeptide present in the systems (Table 1). For all the compositions investigated except 50:0.1 and 75:0.1 (FEFK:E, w:w), di- terta-, hexa- and octapeptides are detected. For $C_0 \leq 75$ mg mL^{-1}, at all enzyme concentrations, the main products are the dipeptide FE and FK (ca. 90 to 96 %) and the higher the enzyme concentration the less octapeptide formed. This suggests that for these systems reverse hydrolysis is the favoured reaction. For $C_0 \geq 100$ mg mL^{-1} lower dipeptide contents and increased amounts of tetra- and octapeptides are detected. For these series, the final octapeptide content is found to increase with increasing peptide to enzyme ratio for a given tetrapeptide concentration. Similarly, for a given enzyme concentration, the higher the initial tetrapeptide concentration the more octapeptide formed for $C_0 \geq 100$ mg mL^{-1}. The results indicate that the gelation kinetic is not solely related to the FEFK/Enzyme molar ratio but rather to a minimal initial tetrapeptide concentration.

Table 1: a) FEFK:E molar ratio investigated; b) octapeptide content after a week incubation.

a

E mg mL^{-1}	FEFK / mg mL^{-1} 50	75	100	200
0.1	30367	45550	60734	1E+05
0.3	10122	15183	20245	40489
0.5	6073	9110	12147	24293

b

E mg mL^{-1}	FEFK / mg mL^{-1} 50	75	100	200
0.1	N/A	N/A	39%	52%
0.3	N/A	0.84%	26%	
0.5	N/A	0.18%	16%	23%

SAXS experiments have been performed to further investigate the structural changes occurring during the fibrillar formation. Fig. 1 shows the scattered intensity curves obtained for our samples at room temperature at discrete time points. As can be seen from Fig. 1a no changes in the scattered intensity are observed over time for C_0=50 mg mL^{-1} consistent with the low level of octapeptide detected by HPLC. For C_0=70 mg mL-1 (Fig 1b) an increase of the scattered intensity over time is observed. This suggests that although self-assembly of octapeptides might occur, their low concentration prevents the formation of fibrillar structure hence gelation of the sample. For $C_0 \geq 100$ mg mL-1, the increase is more pronounced in agreement with the higher level of octapeptides detected by HPLC (Fig 1c). This indicates that the synthesised octapeptide self assembles to form supramolecular structures as observed by SAXS and the scattering profiles shown in Fig. 1 can be used to accurately depict changes in the hydrogel network formation with both changes in peptide and enzyme concentrations. To extract structural information, for $C_0 \geq 100$ mg mL-1 the scattering patterns were fitted using the following functional form corresponding to a generalised Guinier-Porod model[3]:

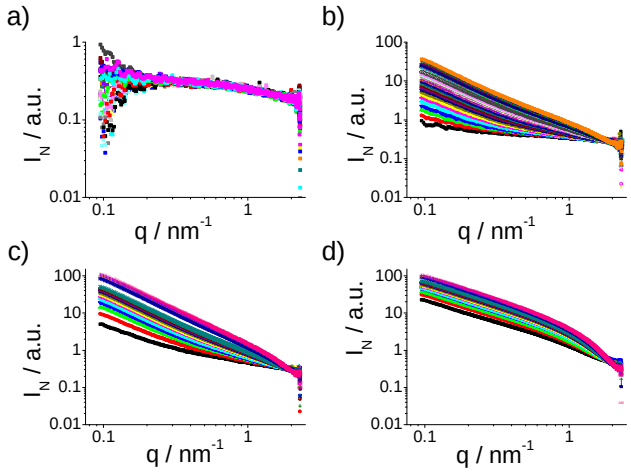

Fig. 1: Scattering curves at discret time point for a) C_0=50 mg mL^{-1}, b) C_0=75 mg mL^{-1}, c) C_0=100 mg mL^{-1} and d) C_0=200 mg mL^{-1}, with an enzyme concentration of 0.5 mg mL^{-1}.

$$I_N(q) = {KCM}/{q^s}\, exp\left(-{q^2 R_g^2}/{3-s}\right) \quad q \leq Q_1 \quad \text{and} \quad I_N(q) = {I_F}/{q^m} \quad q \geq Q_1$$

$$\text{with} \quad Q_1 = {1}/{R_g}\left[{(\alpha - s)(3-s)}/{2}\right]^{1/2}$$

The first term is used to fit the low-q region and corresponds to a generalised Guinier model in which the parameter s allows the modeling of non-spherical objects. For three dimensional globular objects (such as spheres), s = 0 and one recovers the empirical Guinier law. For infinitely long rods s = 1 and for lamellae s = 2, these correspond to the modified Guinier law encounter for such geometry. The fit of the low-q region provides the radius of gyration R_g, the concentration of scattering object C and their molecular weight M – which was fixed to 1120 g mol-1 the average molecular weight of an octapeptide molecule. The second term

is a power law and describes the decay of the scattering intensity in the high-q region. In the framework of fractal analysis, the exponent m can assume values from 1 to 4 relating directly to the fractal characteristics of the scattering objects. When $3 < m < 4$, the scattering can be considered to be the reflection from the surface (interface) of the scattering object. The scattering is said to emerge from a "surface fractal" and the lower the value of m the rougher the surface. For $1 < m < 3$, the scattering originate from a "mass fractal" and the value of the exponent is indicative of the degree of compactness of the scattering object – the lower the value of m the looser the structure.

Good aggreement between the model and the experimental data are found. At all the enzyme concentrations tested, for C_0=100 mg mL^{-1} the dimensionality parameter s assumes value between 1.7 and 1.8 while for C_0=200 mg mL^{-1} s=1.1-1.2. This discrepancy in the dimensionality parameter s points to differences in the structural assembly and can be related to changes in the aspect ratio of the fibres. For C_0=100 mg mL^{-1} the lower value of s may indicate that shorter fibres form. For both C_0=100 and 200 mg mL^{-1}, R_g=1.0-1.1 nm similar to that reported for FEFEFKFK[(1)] irrespectively of the enzyme concentration, suggesting the fibres present similar cross section radius in all cases. Finally the concentration of assembled peptides was derived (Fig 3 a and b). For $C_0 \geq$100 mg mL^{-1}, similar kinetics are observed with a fast rise of concentration at early stage followed by a plateau although differences are apparent.

Much higher concentration in scattering objects, i.e. assembled octapeptides, are noticed for C_0=200 mg mL^{-1} in agreement with the results derived from HPLC. Although similar assembled octapeptide contents are detected at long incubation time (*ca.* 50 mg mL^{-1} after 35 hrs) for the series of sample with C_0=200 mg mL^{-1}, the concentration is found to increase more rapidly at higher enzyme concentration. This suggests that the amount of assembled octapeptide, *i.e.* the kinetics of fibrillar formation, is affected by the enzyme concentration. Likewise the results indicate that a similar equilibrium state is reached within 35 hrs irrespectively of the enzyme concentration.

For C_0=100 mg mL^{-1}, a much lower assembled octapeptide concentration (12 to 17 mg mL^{-1}) is found in line with the HPLC analysis. Although a fast initial rise of concentration is observed for all the enzyme concentrations, it is less pronouced than for C_0=200 mg mL^{-1}. Similarly to C_0=200 mg mL^{-1} series, at early stage (first 7 hrs), the higher the enzyme concentration the faster the kinetics of fibrillar formation. 10 hrs onwards, the concentrations increase at a slower rate and the sample with the lower enzyme concentration exhibits slightly higher concentration in scattering object, i.e. assembled octapeptides. It is also apparent that no equilibrium has been reached after 35 hrs of incubation as an increase in octapeptide concentrations is still observed.

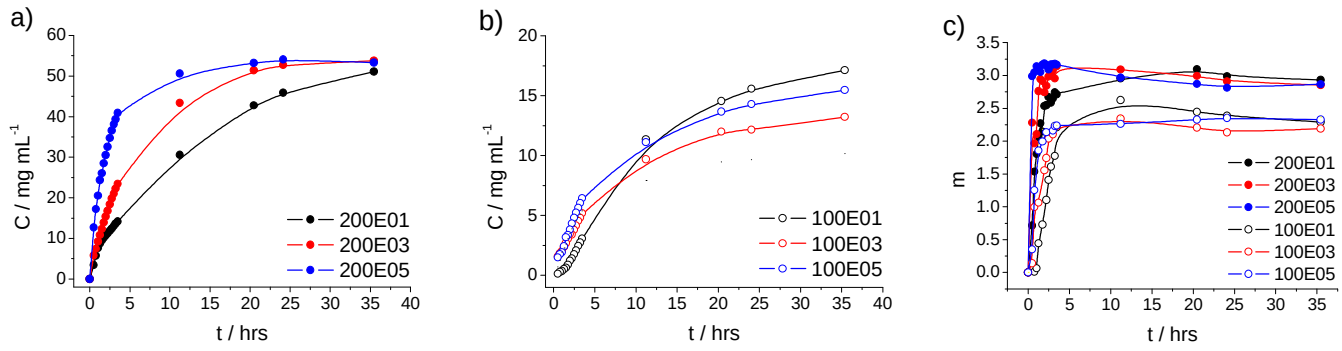

Fig. 2: Time evolution of the concentration in assembled peptide extracted from the general Guinier fit for C_0=200 mg mL^{-1} (a) and C_0=100 mg mL^{-1} (b); an average molecular weight of 1120 g mol^{-1} was used for the fitting. c) Time evolution of the high-q exponent m.

The high-q regime of the scattering pattern was fitted using a power law (Fig 3c). The exponent which relates to the fractal dimension of the system is a measure of the compactness of the hydrogel and it varies with the initial tetrapeptide concentration. For both C_0=100 and 200 mg mL^{-1} and at any enzyme concentration, a sharp increase of the the fractal dimension is observed for the first 3 hrs. 3 hrs onward there is no noticible changes in the value of the high-q exponent and m assumes the values of *ca.* 2.75 for C_0=200 mg mL^{-1} and *ca.* 2.25 for C_0=100 mg mL^{-1}. Such values for the fractal dimension are reminiscent of mass fractal. The higher value observed for C_0=200 mg mL^{-1} indicates an increased compactness/density of the self assembled fibrils that form the local network morphology with increased initial tetrapeptide concentration. This was

expected given the higher octapeptide contents detected for C_0=200 mg mL^{-1} as well as the higher assembled octapeptide contents derived from the Guinier analysis. Finally for a given tetrapeptide concentration, *m* remains unaltered by a change in the enzyme concentration as shown by Fig 3c suggesting similar local network morphology at a length scale $L < 6$ nm.

The analysis of the SAXS patterns provides crucial information about the dimension of the fibres consistuting the network and its local density that are dependent on the initial tetrapeptide and enzyme concentrations. This valuable information on the local nanostructure on different length scales in the reciprocal space (*q*) will be correlated to real space observation (TEM imaging). In turn, the structural information derived from the SAXS analysis may prove key in facilitating the understanding of the relationships between self-assembly behaviour and local nanostructure with final physical properties of the materials.

References:

1. A. Saiani, A. Mohammed, H. Frielinghaus, R. Collins, N. Hodson, C. M. Kielty, M. J. Sherratt and A. F. Miller, *Soft Matter*, 2009, **5**, 193-202.
2. J. B. Guilbaud, E. Vey, S. Boothroyd, A. M. Smith, R. V. Ulijn, A. Saiani and A. F. Miller, *Langmuir*, **26**, 11297-11303.
3. B. Hammouda, *J. Appl. Crystallogr.*, 2010, **43**, 716-719.